FEBS Letters 584 (2010) 4797–4801

journal homepage: www.FEBSLetters.org

Mutations at key pore-lining positions differentiate the water permeability of fish lens aquaporin from other vertebrates

Luisa Calvanese [a], Marialuisa Pellegrini-Calace [b,1], Romina Oliva [c,*]

[a] Department of Chemistry, University "Federico II" of Naples, Via Cintia 45, I-80126, Naples, Italy
[b] EMBL/EBI, The Wellcome Trust Genome Campus, CB10 1SD, Hinxton, Cambridge, United Kingdom
[c] Department of Applied Sciences, University "Parthenope" of Naples, Centro Direzionale Isola C4, I-80143, Naples, Italy

ARTICLE INFO

Article history:
Received 8 July 2010
Revised 17 October 2010
Accepted 27 October 2010
Available online 2 November 2010

Edited by Robert B. Russell

Keywords:
Aquaporin-0
Water transport
Comparative analysis
Molecular modeling
Adaptive evolution
Fish vision

ABSTRACT

Aquaporin-0 (AQP0) is the major integral membrane protein of lens fiber cell and helps to maintain lens transparency by mediating inter-cell adhesion. To shed light on the unexpected higher water transport efficiency of killifish AQP0 as compared to mammalian orthologues, we performed a comparative analysis of all available AQP0 sequences and built 3D-models for representatives of different vertebrate classes.

The analysis shows that air-living organisms evolved specific mutations at pore-lining positions to modulate the AQP0 water transport efficiency while maintaining the correct tertiary/quaternary arrangement to allow the formation of "thin junctions" between lens fiber cells. We conclude that the low permeability of mammalian AQP0 is required not to promote cell adhesion, but to modulate the water balance in a dry environment.

1. Introduction

Aquaporin-0 (AQP0) is the major membrane protein of fiber cells in eye lens, accounting for >60% of the protein complement of fiber cell membrane in bovine [1]. AQP0 is believed to play a key role in maintaining a healthy functional lens by regulating water permeation across the fiber cell plasma membrane. It has also been demonstrated that mammalian AQP0 has adhesive properties and forms the "thin junctions" between lens fiber cells, which consist of 11–13 nm thick square AQP0 arrays. This maintains the lens transparency [2]. The AQP0 physiological importance is also underscored by the observation that specific mutations lead to cataract formation (reviewed in [3]).

Interestingly, bovine AQP0 water conductance is at least 15-fold lower than that of "orthodox" aquaporins, i.e., aquaporins with high and specific selectivity to water, such as the red blood cell aquaporin-1 (AQP1) [4,5]. The biological significance and structural determinants of the unusually low permeability of mammalian AQP0 have not yet been fully understood [6–10].

Before the experimental 3D-structure of any aquaporin was made available, Virkki and colleagues cloned and functionally characterized AQP0 from the killifish *Fundulus heteroclitus*, the first aquaporin from fish [11]. Unexpectedly, the killifish AQP0 showed a water permeability significantly higher than mammalian AQP0s and comparable to that of AQP1. However, the sequence and structural features determining its high water permeability could not be clarified at the time.

Today experimental 3D-structures at atomic detail are available for 10 aquaporin subfamilies, including bovine and sheep AQP0 [6,7]. All of them are homotetramers with each monomer, defining a single pore for passive diffusion, characterized by two constrictions. The former one is located around the asparagines of two conserved NPA (Asn-Pro-Ala) motifs, at the middle of the channel. The latter and narrower constriction, known as aromatic/Arg (ar/R) selectivity filter, is found at the periplasmic side of the channel and is formed by four residues including aromatic amino acids and a widely conserved arginine. As compared to AQP1 and other aquaporins, the 3D structures of AQP0 show an additional constriction, at the cytoplasmic side of the channel, formed by residues His66, Phe75 and Tyr149 (sequence numbering from bovine AQP0) [12]. Furthermore, in the periplasmic vestibule the side-chain of Tyr23 protrudes into the pore. Molecular dynamics (MD) studies have shown that Tyr23 and Tyr149 may act as major

* Corresponding author. Fax: +39 (0)81 5476514.
E-mail address: romina.oliva@uniparthenope.it (R. Oliva).
[1] Present address: Department of General and Environmental Physiology, University of Bari, Via Amendola 165/A, I-70126 Bari, Italy.

0014-5793/$36.00
doi:10.1016/j.febslet.2010.10.058

Table 1
25 AQP0 sequences with relative accession number, species, taxonomic class and PDB-code (when experimental 3D structures are available). The species common name is also given, when used in the text. The 19 representative sequences shown in Fig. S2 are in bold.

Accession number	Species	Class/superclass	PDB-code
ref|NP_036196	***Homo sapiens***	**Mammalia**	**–**
ref|XP_001115118	***Macaca mulatta***	**Mammalia**	**–**
ref|NP_001074369	***Canis lupus familiaris***	**Mammalia**	**–**
ref|NP_001099189	***Rattus norvegicus***	**Mammalia**	**–**
gb|ABY47997	***Cavia porcellus***	**Mammalia**	**–**
ref|NP_032626	***Mus musculus***	**Mammalia**	**–**
gb|AAH82567	*Mus musculus*	Mammalia	–
ref|XP_001504894	***Equus caballus***	**Mammalia**	**–**
ref|NP_001153230	***Ovis aries* (sheep)**	**Mammalia**	**1sor, 2b6o**
ref|NP_001093431	***Oryctolagus cuniculus***	**Mammalia**	**–**
ref|NP_776362	***Bos taurus* (bovine)**	**Mammalia**	**1ymg, 2b6p, 2c32**
ref|NP_989597	***Gallus gallus* (chicken)**	**Aves**	**–**
ref|NP_001088304	***Xenopus laevis***	**Amphibia**	**–**
pir||JN0557	*Xenopus laevis*	Amphibia	–
ref|NP_001090816	***Xenopus tropicalis***	**Amphibia**	**–**
sp|Q06019	***Rana pipiens***	**Amphibia**	**–**
ref|NP_001003534	***Danio rerio* (zebrafish)**	**Actinopterygii/osteichthyes**	**–**
gb|AAH98535	*Danio rerio* (zebrafish)	Actinopterygii/osteichthyes	–
ref|NP_001018356	*Danio rerio* (zebrafish)	Actinopterygii/osteichthyes	–
gb|AAI55723	*Danio rerio* (zebrafish)	Actinopterygii/osteichthyes	–
dbj|BAH98062	***Neoceratodus forsteri* (Australian lungfish)**	**Sarcopterygii/osteichthyes**	**–**
dbj|BAH98061	***Protopterus annectens* (African lungfish)**	**Sarcopterygii/osteichthyes**	**–**
emb|CAG07459	***Tetraodon nigroviridis* (pufferfish)**	**Actinopterygii/osteichthyes**	**–**
emb|CAG04065	*Tetraodon nigroviridis* (pufferfish)	Actinopterygii/osteichthyes	–
gb|AAF04146	***Fundulus heteroclitus* (killifish)**	**Actinopterygii/osteichthyes**	**–**

determinants of the low water permeability of bovine AQP0, with Tyr23 in particular being responsible for the largest local barrier to water passage [13,14]. Mutation of Tyr23 to its AQP1 counterpart Phe has also been shown by MD simulations to lead to a two to fourfold enhancement in AQP0 water permeability [14]. More recently, we have investigated the effect of these two tyrosine residues on the electrostatic potential of the bovine AQP0 channel, showing that both Tyr23 and Tyr149 severely affect the channel's electrostatic profile. In particular Tyr149 is responsible for a deep electrostatics minimum at the cytoplasmic side of the AQP0 channel, at variance with the rather flat cytoplasmic electrostatic profile of canonical aquaporins. Interestingly upon the in silico mutation of Tyr149 to the AQP1 Thr, an "orthodox-like" electrostatic profile was restored [15].

Furthermore, the 3D-structure of sheep AQP0 shed light on the structural basis of thin junction formation. It was solved by electron crystallography first at 3 Å [8] and then at 1.9 Å resolution [6] from large double-layered 2D crystals and reproduced the dimensions of the thin junctions between lens fiber cells. In the crystals two opposing tetramers interact with each other via their extracellular domains. This interaction is facilitated by the fairly flat AQP0 extracellular surface, which, differently from other aquaporins, lacks bulky extracellular loops and glycosylation [1] and allows specific contacts mediated by corresponding extracellular loops in opposing AQP0 molecules [6,8,12,16].

Today, AQP0 sequences from several classes of vertebrates (mammalia, aves, amphibia and bony fish) are also available. To get insight into the difference in the water transport efficiency observed between fish and other vertebrates AQP0, we performed a comparative analysis of all available AQP0 sequences. In order to better investigate the differences on a structural basis, we also built three-dimensional models for representatives of each vertebrate class. On the basis of this sequence and structure analysis, we emphasize a common character of the pore within each group of vertebrates and illuminate the structural determinants differentiating fish AQP0 from other vertebrates. Moreover, our results suggest that AQP0 has adaptively evolved to maintain a high water content in the eye lens cells of air-living creatures.

2. Materials and methods

For details on the sequences collection and analysis, model building and electrostatic potential calculations see Supplementary materials and Oliva et al. [15].

3. Results and discussion

Accession numbers, source and taxonomic class of the 25 sequences available for AQP0, all from vertebrates, are reported in Table 1. (For a multiple alignment see Fig. S1). The average inter-pair sequence identity among them is 75%. This result is comparable to the average inter-pair sequence identity, 79%, found for the other 22 aquaporin subfamilies for which representative sequences are available from the SwissProt database [17]. Despite the overall similarity between AQP0 sequences belonging to different vertebrate classes, a distinctive profile emerges for the residues lining the pore of each of the three groups: mammals, amphibians and fish. This can be easily appreciated from their pore-logo representations shown in Fig. 1B, that we derived for each vertebrates class from the 51 alignment positions occupied by pore-lining residues. Please note that in the pore-logo representations, amino acids are ordered geometrically along the channel axis, i.e. adjacent amino acids are not necessarily adjacent in the sequence, but they lie adjacent in the channel, giving a direct view of the composition of the pore [18]. (For the correspondence between sequence and pore-logo numbers, see Fig. S2). As it can be seen from Fig. 1B, amino acids at the pore-lining positions are strictly conserved within mammals and amphibians with exceptions at few positions (15, 21 and 22 for mammals and 9, 20, 26, 40 for amphibians), which still show a limited variability and host conservative substitutions. The fish AQP0 pore-logo also shows a limited variability, mostly concentrated in the periplasmic vestibular region.

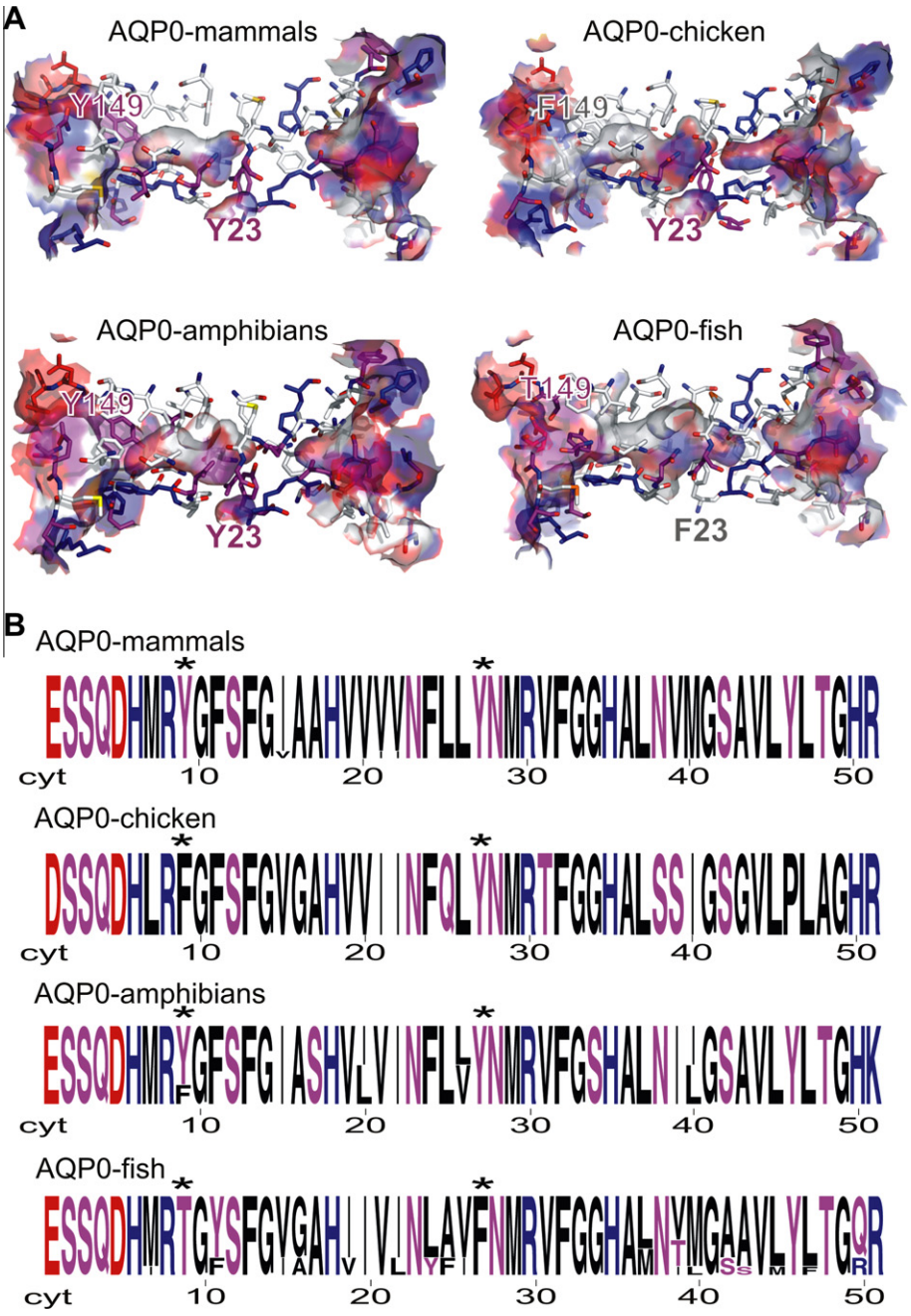

Fig. 1. Representation of sequence and structural features of the pores. Each pore is orientated from the intracellular (left) to the extracellular (right) side. Acidic residues are colored in red, basic residues in blue and polar residues in purple. (A) 3D-Structure representation: for each structure, all the residues lining the pore are shown. (B) Sequence representation: pore-lining residues are shown as pore-logos for all the sequences belonging to the corresponding taxonomic class. Note that logo numbers correspond to the structural position of the residues along the channel axis and not to their sequence position. For the corresponding sequence position refer to Fig. S2.

Differences in the pore-logos of the different AQP0 vertebrate classes are the result of specific amino acid substitutions at key pore-lining positions. They are listed in Table 2, ordered according to their location along the channel axis, from the cytoplasmic to the periplasmic side. To clarify the structural effect of such amino acid substitutions, three-dimensional models for killifish AQP0, *Rana pipiens* AQP0 and *Gallus gallus* AQP0, as representatives of fish, amphibians and aves, respectively, have been built and compared with the AQP0 bovine 3D-structure at 2.24 Å resolution [7]. A representation of the three pores from the corresponding 3D model or structure is shown in Fig. 1A, together with the pore-logo representation for each vertebrate group. By a visual inspection, it is apparent that the substitution of several pore-lining residues results in different pore diameters. Overall, at both the periplasmic and cytoplasmic sides, the fish AQP0 channel is wider than the bovine, frog and chicken ones. In Fig. 2, the pore diameters estimated by PoreWalker [19] are shown for bovine and fish AQP0 channels, together with a stick representation of the pore-lining residues listed in Table 2 and the pore diameters of bovine AQP1, for comparison. Bovine AQP0 is narrower than fish AQP0 at the cytoplasmic side, in correspondence of the cytoplasmic constriction site given by residues Phe75, His66 and Tyr149 (logo positions: 11, 18 and 9). In fish, Tyr149 and Phe75 are substituted by a smaller Thr149 and a slightly larger Tyr75, leading to a consequent diameter

Table 2
Identity of residues at key pore-lining positions.

Sequence position[a]	Logo position	Pore height (Å)	Mammals	Amphibians	Fish	Chicken
66	6	~−12	His	His	His	His
149	9	~−12	Tyr	Tyr (3)/Phe (1)	Thr	Phe
75	11	~−12	Phe	Phe	Tyr(7)/ Phe(2)	Phe
141	24	~−3	Phe	Phe	Leu(7)/ Tyr(2)	Phe
52	25	~−3	Leu	Leu	Ala(7)/ Phe(2)	Gln
168	26	~3	Leu	Leu(2)/ Val(2)	Val(7)/ Leu(2)	Leu
23	27	~3	Tyr	Tyr	Phe	Tyr

[a] To be scaled by +1 for *X. laevis* and *X. tropicalis*.

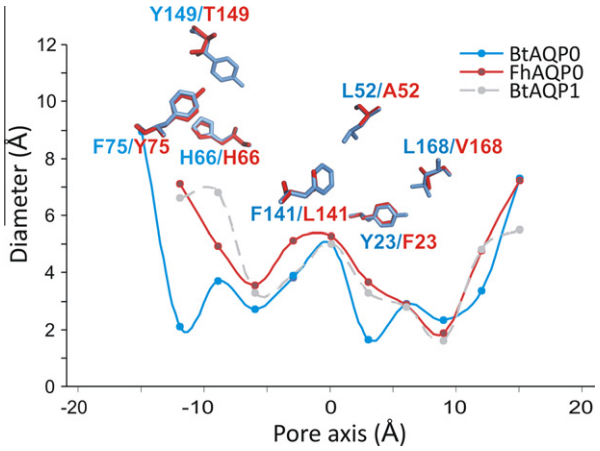

Fig. 2. Diameter profiles calculated by PoreWalker [19] for the channels of bovine (light blue) and killifish AQP0 (red); residues whose mutation is responsible for the different size at the different pore heights are shown in a stick representation. The pore diameters of bovine AQP1 (gray) are also reported, for comparison.

increase of ~5 Å. At the NPA constriction, mammalian and amphibian channels are ~1 Å larger than the fish pore due to their Phe141 and Leu52 (logo positions 24 and 25) substituted by smaller Leu141 and Ala52, respectively, in killifish. At the periplasmic side of the NPA region, mammalian Tyr23 (logo position 27 and pore height 3 Å) is substituted by Phe23 in fish; moreover the mammalian Leu168 (logo position 26) is substituted by a Val in killifish. This double mutation results in a ~2 Å increase in the corresponding pore diameter.

Residues at positions 23 and 149 are expected to play a major role in determining peculiar AQP0 permeability properties. Several lines of evidence indeed suggest that Tyr23 (logo position 27) and Tyr149 (logo position 9) may be associated to the low water conductance of mammalian AQP0 [13–15], and that their mutation to the corresponding AQP1 residues, Phe23 and Thr149, tends to restore dynamic and electrostatic features characteristic of orthodox aquaporins [14,15].

From our analysis it clearly emerges that Tyr23 and Tyr149 are conserved among mammalian and amphibian AQP0 sequences available, but are substituted by AQP1-like Phe and Thr residues, respectively, in fish. This contributes to explain the unexpected high water conductance measured for killifish AQP0 [11]. AQP0 from *G. gallus* also presents a tyrosine at position 23, analogously

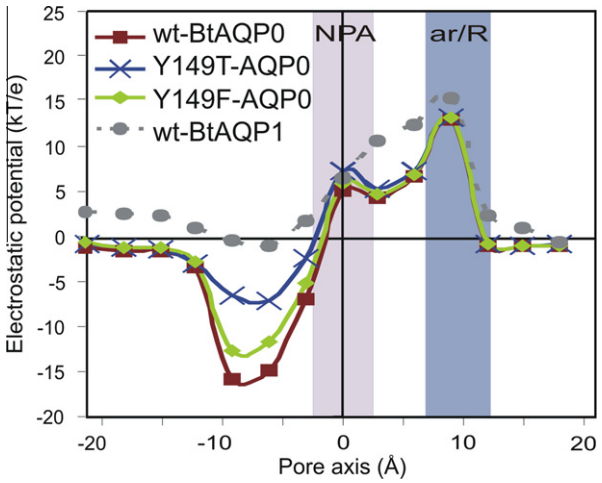

Fig. 3. Electrostatic potential calculated at pore centers for the BtAQP0 Y149F mutant. Electrostatic potentials are also shown for wt BtAQP0, its Y149T mutant and wt BtAQP1 from [15], for comparison.

to mammals and amphibians. Interestingly, at position 149 both *G. gallus* and *Xenopus tropicalis* exhibit a Phe residue, at variance with all other vertebrates. To investigate the effect of this substitution, we calculated here the channel electrostatic profile for the bovine AQP0 (BtAQP0) Y149F mutant. It is shown in Fig. 3, together with those of wild-type BtAQP0, of its Y149T mutant and of wild-type BtAQP1, previously reported in [15], for comparison. From Fig. 3 it is apparent that the Y149F mutation tends to restore a flat "orthodox"-like trend at the cytoplasmic side of the channel. However, its effect is smaller than that of the Y149T substitution. Therefore, the minor effect on both the size and electrostatic features of the channel suggests that this mutation is not expected to dramatically affect the water conductance properties of *G. gallus* and *X. tropicalis* AQP0, as compared to mammals and other amphibians.

As for AQP0 adhesion properties, it is noteworthy that the identity of residues involved in the AQP0 junction formation, Pro109, Arg113, Pro38, Arg33, Trp34 [16], is conserved within all the analysed AQP0 sequences, with only Arg33 mutated to Lys33 in the four amphibian sequences. Pro110 represents an exception since it is substituted in amphibians, fish and chicken by a smaller amino acid, like Asn, Ala, Thr, Ser or Gly. However, we note that Pro110 is less involved than Pro38 and Pro109 in the inter-tetramer contacts, and its substitution by a small Ala or Asn residue, in amphibians and fish, respectively, is consequently not expected to seriously affect their adhesion properties. In addition, the length and conformation of extracellular loops is preserved in fish AQP0, resulting in a flat extracellular surface which allows two opposing tetramers to approach each other and give adhesion by making specific contacts, strictly similar to those observed for sheep AQP0 by Gonen et al. [6,8,12] (see Fig. S3).

Staying on the issue of lens transparency, it is also interesting that single amino acids whose mutation is correlated to congenital cataracts are all strictly conserved among the analysed AQP0 sequences (for details see Supplementary materials).

4. Conclusions

From our comparative analysis, the high water permeability of killifish AQP0 [11] clearly emerges as a consequence of its pore composition, which is common to all known fish AQP0s. Note that fish species in our sample are quite various. They are mostly fresh

water fish, with putterfish and killifish being euryhaline, i.e. able to live both in fresh and brackish waters, and include Australian lungfish, which is considered one of the oldest living vertebrate genera on the planet [20]. Therefore, it appears that air-living organisms, including amphibians, have recently evolved specific mutations to restrict the water permeability of their lens aquaporin. Possibly this was an evolutionary adaptation, acquired together with the macroscopic phenotype of eyelid appearance, to guarantee the maintenance of eye humidity and avoid sudden loss of water in a dry environment.

The reduced permeability of the air-living organisms AQP0 can be confidently correlated with both the identity of residues at positions 23 and 149 and the effect they have on the electrostatics [15] and dynamics [13,14] of the channels, and an overall reduced size of the channel, due to mutations at several pore-lining positions. The mercurials-sensitivity and regulation by pH seem also to be at some extent class-dependent (see Supplementary materials). On the contrary, the fish AQP0 structure and sequence are perfectly compatible with the maintenance of an integer junctional form, very similar to that observed for mammalian AQP0 (Fig. S3). In fact, the eye lens is transparent in both fish and air-living organisms.

Our main finding is therefore that AQP0 from air-living vertebrates accumulated specific pore mutations, while maintaining the overall sequence similarity to the AQP0 subfamily and the correct tertiary and quaternary structural arrangement to allow the formation of "thin junctions" between lens fiber cells. On these bases, the low permeability of mammalian AQP0 to water appears to be an evolutionary strategy not to promote cell adhesion, as recently proposed [13], but to modulate the water balance in a completely different environment, as compared to aquatic organisms.

This can have intriguing consequences in the physiology of fish vision as compared to air-living organisms and should be kept in mind when using fish models as tools for understanding the biology of visual disorders in humans [21,22].

Acknowledgements

We thank Prof. Janet M. Thornton and Dr. Mariella Ferrante for helpful discussions. R.O. and M.P.C. were supported by the FEBS Short-Term Fellowships programme. M.P.C. was funded by the UK BBSRC grant number BBE0226421.

Appendix A. Supplementary data

Supplementary data associated with this article can be found, in the online version, at doi:10.1016/j.febslet.2010.10.058.

References

[1] Broekhuyse, R.M., Kuhlmann, E.D. and Stols, A.L. (1976) Lens membranes II. Isolation and characterization of the main intrinsic polypeptide (MIP) of bovine lens fiber membranes. Exp. Eye Res. 23, 365–371.
[2] Costello, M.J., McIntosh, T.J. and Robertson, J.D. (1989) Distribution of gap junctions and square array junctions in the mammalian lens. Invest. Ophthalmol. Vis. Sci. 30, 975–989.
[3] Chepelinsky, A.B. (2009) Structural function of MIP/aquaporin 0 in the eye lens; genetic defects lead to congenital inherited cataracts. Handb. Exp. Pharmacol. 265, 97.
[4] Chandy, G., Zampighi, G.A., Kreman, M. and Hall, J.E. (1997) Comparison of the water transporting properties of MIP and AQP1. J. Membr. Biol. 159, 29–39.
[5] Yang, B. and Verkman, A.S. (1997) Water and glycerol permeabilities of aquaporins 1-5 and MIP determined quantitatively by expression of epitope-tagged constructs in Xenopus oocytes. J. Biol. Chem. 272, 16140–16146.
[6] Gonen, T., Cheng, Y., Sliz, P., Hiroaki, Y., Fujiyoshi, Y., Harrison, S.C. and Walz, T. (2005) Lipid–protein interactions in double-layered two-dimensional AQP0 crystals. Nature 438, 633–638.
[7] Harries, W.E., Akhavan, D., Miercke, L.J., Khademi, S. and Stroud, R.M. (2004) The channel architecture of aquaporin 0 at a 2.2-Å resolution. Proc. Natl. Acad. Sci. USA 101, 14045–14050.
[8] Gonen, T., Sliz, P., Kistler, J., Cheng, Y. and Walz, T. (2004) Aquaporin-0 membrane junctions reveal the structure of a closed water pore. Nature 429, 193–197.
[9] Han, B.G., Guliaev, A.B., Walian, P.J. and Jap, B.K. (2006) Water transport in AQP0 aquaporin: molecular dynamics studies. J. Mol. Biol. 360, 285–296.
[10] Hashido, M., Ikeguchi, M. and Kidera, A. (2005) Comparative simulations of aquaporin family: AQP1, AQPZ, AQP0 and GlpF. FEBS Lett. 579, 5549–5552.
[11] Virkki, L.V., Cooper, G.J. and Boron, W.F. (2001) Cloning and functional expression of an MIP (AQP0) homolog from killifish (Fundulus heteroclitus) lens. Am. J. Physiol. Regul. Integr. Comp. Physiol. 281, R1994–R2003.
[12] Gonen, T. and Walz, T. (2006) The structure of aquaporins. Q. Rev. Biophys. 39, 361–396.
[13] Jensen, M.O., Dror, R.O., Xu, H., Borhani, D.W., Arkin, I.T., Eastwood, M.P. and Shaw, D.E. (2008) Dynamic control of slow water transport by aquaporin 0: implications for hydration and junction stability in the eye lens. Proc. Natl. Acad. Sci. USA 105, 14430–14435.
[14] Qiu, H., Ma, S., Shen, R. and Guo, W. (2010) Dynamic and energetic mechanisms for the distinct permeation rate in AQP1 and AQP0. Biochim. Biophys. Acta. 1798, 318–326.
[15] Oliva, R., Calamita, G., Thornton, J.M. and Pellegrini-Calace, M. (2010) Electrostatics of aquaporin and aquaglyceroporin channels correlates with their transport selectivity. Proc. Natl. Acad. Sci. USA 107, 4135–4140.
[16] Engel, A., Fujiyoshi, Y., Gonen, T. and Walz, T. (2008) Junction-forming aquaporins. Curr. Opin. Struct. Biol. 18, 229–235.
[17] Apweiler, R. et al. (2004) UniProt: the Universal Protein knowledgebase. Nucleic Acids Res. 32, D115–D119.
[18] Oliva, R., Thornton, J.M. and Pellegrini-Calace, M. (2009) PoreLogo: a new tool to analyse, visualize and compare channels in transmembrane proteins. Bioinformatics 25, 3183–3184.
[19] Pellegrini-Calace, M., Maiwald, T. and Thornton, J.M. (2009) PoreWalker: a novel tool for the identification and characterization of channels in transmembrane proteins from their three-dimensional structure. PLoS Comput. Biol. 5, e1000440.
[20] Allen, G.R., Midgley, S.H. and Allen, M. (2002) in: Field Guide to the Freshwater Fishes of Australia (Knight, Jan and Bulgin, Wendy, Eds.), pp. 54–55, Western Australia Museum, Perth, W.A..
[21] Goldsmith, P. and Harris, W.A. (2003) The zebrafish as a tool for understanding the biology of visual disorders. Semin. Cell Dev. Biol. 14, 11–18.
[22] McMahon, C., Semina, E.V. and Link, B.A. (2004) Using zebrafish to study the complex genetics of glaucoma. Comp. Biochem. Physiol. C Toxicol. Pharmacol. 138, 343–350.